



HAL
open science

Uncovering the behavior of screen-printed carbon electrodes modified with polymers molecularly imprinted with lipopolysaccharide

Bianca Elena Stoica, Ana-Mihaela Gavrilă, Andrei Sarbu, Horia Iovu, Hugues Brisset, Andreea Miron, Tanta-Verona Iordache

► To cite this version:

Bianca Elena Stoica, Ana-Mihaela Gavrilă, Andrei Sarbu, Horia Iovu, Hugues Brisset, et al.. Uncovering the behavior of screen-printed carbon electrodes modified with polymers molecularly imprinted with lipopolysaccharide. *Electrochemistry Communications*, 2021, 124, pp.106965. 10.1016/j.elecom.2021.106965 . hal-03406104

HAL Id: hal-03406104

<https://hal.science/hal-03406104>

Submitted on 27 Oct 2021

HAL is a multi-disciplinary open access archive for the deposit and dissemination of scientific research documents, whether they are published or not. The documents may come from teaching and research institutions in France or abroad, or from public or private research centers.

L'archive ouverte pluridisciplinaire **HAL**, est destinée au dépôt et à la diffusion de documents scientifiques de niveau recherche, publiés ou non, émanant des établissements d'enseignement et de recherche français ou étrangers, des laboratoires publics ou privés.



Uncovering the behavior of screen-printed carbon electrodes modified with polymers molecularly imprinted with lipopolysaccharide

Bianca Elena Stoica^{a,c,1}, Ana-Mihaela Gavrilă^{a,1}, Andrei Sarbu^a, Horia Iovu^c, Hugues Brisset^b, Andreea Miron^a, Tanta-Verona Iordache^{a,*}

^a Chemistry and Petrochemistry ICECHIM, spl. Independentei 202, Bucharest 060021, Romania

^b Laboratoire MAPIEM, Université de Toulon, CS 60584, Toulon Cedex 983041, France

^c APM Group, Faculty of Applied Chemistry and Materials Science, University POLITEHNICA of Bucharest, Gh. Polizu 1-7, Bucharest 011061, Romania

ARTICLE INFO

Keywords:

Modified screen-printed carbon electrodes
Lipopolysaccharides
Molecularly imprinted polymers
Electrochemical detection

ABSTRACT

In the context of global issues concerning pathogen contamination of surface and ground waters, this pioneering study describes the fabrication of screen-printed carbon electrodes modified with polymers molecularly imprinted with lipopolysaccharide in an attempt to detect endotoxins derived from specific Gram-negative bacteria. The biosensors detected lipopolysaccharides derived from *Pseudomonas Aeruginosa* with high specificity, relative to control sensors, while the response to the same endotoxin derived from *Escherichia coli* was quite different.

1. Introduction

Microbiological contamination is an important problem affecting water quality worldwide. Pathogens are normal components of all ecosystems, but microbiological contamination with faecal bacteria following anthropogenic activity is considered to be a crucial problem in all aquatic environments [1]. Gram-negative bacteria (GNB) are among the most significant threats, causing health problems for the human population due to antibiotic resistance [2]. Therefore, many studies have focused on developing methods for detection of pathogenic bacteria [3]. Although some of the methods are very specific and rapid (for instance the polymerase chain reaction, PCR method, delivers results within 1 h), the sample preparation protocols are cumbersome.

In recent years, there has been great interest in the development of sensors for detecting toxic lipopolysaccharides (LPS), which compose the outer membrane of GNB [4–6]. Cho et al. developed an electrochemical sensor using a gold electrode modified using a metal complex, Cu²⁺ and nitrilotriacetic acid, to bond the O-side chain of LPS from *E. coli* [4]. Li et al. reported an electrochemical sensor based on a dual functional Cu²⁺-modified metal-organic framework for LPS detection from *E. coli* (via binding to C18 alkane thiol chains) [5]. Jiang et al. presented a miniaturized paper-supported 3D cell-based electrochemical sensor for in situ detection of nitric oxide (released from mouse

macrophage cells after treatment with LPS from *Salmonella enterica*) [6]. The electrochemical sensors prepared by these various techniques were sensitive for LPS (with LODs around 0.01 ng LPS/mL), yet specificity towards different types of LPS was not proven. In this regard, molecular imprinting (MI) can be of use.

Molecularly imprinted biosensors have emerged as reliable devices for detecting not only small molecules (with a molecular mass less than 1 kDa) but also biomacromolecules [7–10]. The MI technique generally offers simplicity and cost-efficiency, but molecularly imprinted polymers (MIPs) also present important improvements in stability, reusability, specificity and selectivity, compared to the conventional products used for biosensor design [11,12]. Recent MI approaches in biosensor design for bacteria detection are based on whole cell imprinting [13–15]. However, these approaches impose certain working conditions, due to bacteriological hazards, which can be an impediment for biosensor manufacturers. As a result, the aim of this study was to provide a simpler and more promising method for signaling the presence of GNB in aqueous systems by detecting LPS. Furthermore, this endotoxin released after bacterial death causes various inflammatory symptoms and physiological disorders [16]. Hence, the quick detection of dangerous amounts of LPS in aqueous systems would be helpful in promoting on-site measures to prevent the further contamination of water bodies.

* Corresponding author.

E-mail address: tanta-verona.iordache@icechim.ro (T.-V. Iordache).

¹ Authors with equal contribution.

For this purpose, screen-printed carbon electrodes (SPCE) were modified with MIP thin films able to recognize and rebind the bacterial endotoxins (LPS) derived from *Pseudomonas Aeruginosa*. After the previous success of some of the authors in producing LPS-MIP active surfaces for retaining GNB in wastewaters [17], a similar sol-gel derived technique was applied in this work for modifying SPCEs. This procedure makes it possible to dope the mixture with electroactive particles such as zinc oxide (ZnO), with the precursor solution dripped directly onto the SPCE using the drop-casting method [7]. In the present study, the precursor solution also contained an equimolecular mixture of two silane monomers, 3-(2-trimethoxysilyl)-propylmethacrylate (MAPTES) and tetraethyl orthosilicate (TEOS) to ensure adhesion of the LPS-MIP film to the carbon substrate.

2. Experimental section

2.1. Materials

3-(2-Trimethoxysilyl)-propylmethacrylate (MAPTES, 98%, Sigma Aldrich), tetraethyl orthosilicate (TEOS, 98%, Sigma Aldrich), ammonium hydroxide solvent (NH₄OH, 25%, ChimReactive), ethanol (EtOH, 99.6%, Fisher Scientific) and zinc oxide (ZnO, 98% purity, 2 μm, Sigma Aldrich) were used as received. The template molecule was a lipopolysaccharide from *Pseudomonas Aeruginosa* 10 (LPS, 500,000 U.E./mg, 1 E.U. ~0.1 ng endotoxin, Sigma Aldrich), in the form of a lyophilized powder. The carbon screen-printed electrodes C-110 ("3 in 1" electrodes 3.4 × 1 × 0.05 cm in size (l × w × h) and 0.11 cm² geometric area which include the carbon working electrode, a carbon auxiliary electrode and a silver reference electrode) were produced by Metrohm (Romania). We also used a phosphate buffer solution (PBS, pH 7.4, Fisher), potassium chloride salt (KCl, Sigma Aldrich), redox couple potassium ferricyanide (K₃[Fe(CN)₆], Scharlau) and potassium ferrocyanide (K₄[Fe(CN)₆]·3H₂O, Scharlau) and deionized water. Lipopolysaccharide from *Escherichia coli* (O111: B4, 500,000 U.E./mg, 1 E.U. ~0.1 ng endotoxin, Sigma Aldrich) was used for selectivity tests.

2.2. Instrumentation

Cryo-TEM micrographs were acquired on a Tecnai™ G2 F20 TWIN Cryo-TEM (FEI Company). SEM micrographs were recorded on an Environmental Scanning Electron Microscope – Fei Quanta 200. Brunauer-Emmett-Teller (BET) and Barrett-Joyner-Halanda (BJH) methods were used to determine the pore structure of the films by nitrogen adsorption on NOVA 2200 Quantachrome analyser. The water used for LPS extraction and washing was analyzed using a Thermo Scientific™ Evolution™ 260 Bio UV-Vis spectrometer. The cyclic voltammograms (CVs) were acquired using a PGST204 potentiostat/galvanostat system from Metrohm. CVs were recorded in the potential range –0.2 V to 1.2 V relative to the reference electrode, with a scan speed of 100 mV/s and six scan cycles, at room temperature, for three series of sensors. The electrolyte solution contained 0.01 M K₃[Fe(CN)₆]/K₄[Fe(CN)₆] and 0.1 M KCl in PBS at pH 7.4.

2.3. Synthesis of LPS-MIP-SPCE and NIP-SPCE

In a typical batch, two solutions were prepared separately. The precursor solution contained an equimolecular mixture of MAPTES (0.05 mL) and TEOS (0.047 mL) dissolved in 0.5 mL of ethanol at room temperature. The template, LPS (0.25 mg), was solubilized in deionized water (0.25 mL) to yield an equivalent concentration of 500,000 E.U./mL and added to the precursor solution. The catalytic medium for the hydrolysis reaction was 0.283 mL 25% NH₄OH, with a doping agent, zinc oxide (50 wt% relative to the content of MAPTES and TEOS) also added. The precursor solution was gradually poured into the catalytic medium and magnetically stirred at 200 rpm. After 15 min (hydrolysis reaction), the precursor mix was dropped with a syringe directly onto

the SPCE. The LPS-MIP-SPCEs were cured (polycondensation of sols) for 24 h at room temperature followed by aging for 8 h in an oven at 55 °C. In order to obtain quantifiable results, non-imprinted SPCEs (denoted NIP-SPCEs) were prepared as controls using the same methodology described for the LPS-MIP-SPCEs but without the addition of LPS.

3. Results and discussion

3.1. Morphology and porosity of the LPS-MIP

Cryo-TEM analysis of the precursor solution was performed to check whether the mechanism of LPS and monomer auto-assembly is reproducible when using TEOS (Fig. 1). The precursor solution was inspected in the following sequence: aqueous solution of LPS, aqueous solution of LPS + MAPTES, and aqueous solution of LPS + equimolecular mixture of MAPTES and TEOS. Combining LPS with MAPTES leads to the formation of vesicles, which in the presence of TEOS merge and form sols. Compared to the reference NIP-SPCE, the SEM micrographs of LPS-MIP-SPCE revealed a more homogenous deposition and denser pore channeling (Fig. 2), with bigger sol particles as a result of the monomer-LPS auto-assembly.

Brunauer-Emmett-Teller (BET) and Barrett-Joyner-Halanda (BJH) methods were used to determine the pore structure of the LPS-MIP/NIP films. Although the pore diameter was lower for the LPS-MIP film, the surface area, pore surface area and the pore volume were greater than the corresponding values for the NIP (surface area $0.66 \pm 0.10 \text{ m}^2 \text{ g}^{-1}$, pore surface area $1.30 \pm 0.02 \text{ m}^2 \text{ g}^{-1}$ and pore volume $1.69 \cdot 10^{-3} \pm 0.52 \cdot 10^{-3} \text{ m}^3 \text{ g}^{-1}$). This was clear evidence that a denser pore structure with small (interconnected) pores was formed, as indicated by the SEM analyses. After removing the LPS from the structure of the LPS-MIP film, increases in the surface area (from 1.40 ± 0.05 to $1.80 \pm 0.09 \text{ m}^2 \text{ g}^{-1}$), the pore surface area (from 1.60 ± 0.04 to $3.72 \pm 0.05 \text{ m}^2 \text{ g}^{-1}$) and the pore volume (from $2.48 \cdot 10^{-3} \pm 0.59 \cdot 10^{-3}$ to $3.60 \cdot 10^{-3} \pm 0.56 \cdot 10^{-3} \text{ m}^3 \text{ g}^{-1}$) were observed, linking this event to the cleavage of imprinted cavities and the formation of active binding sites.

3.2. Electrochemical behavior of the LPS-MIP-SPCEs

One of the most interesting discoveries in this study was the electrochemical behavior of the LPS-MIP-SPCEs, which was corroborated by the morphology of films and their porosity. Removal of the LPS template from the LPS-MIP-SPCE was achieved by successive washing with ultrapure water. Less time was needed to wash the NIP-SPCE, as there was no LPS to extract in the first step. Following this procedure, the LPS-MIP/NIP-SPCEs were tested for specificity (using LPS from *Pseudomonas Aeruginosa*), washed again with ultrapure water to remove adsorbed LPS molecules and then tested for selectivity against LPS from *Escherichia coli*.

The cyclic voltammograms (CVs) of ferricyanide/ferricyanide in a phosphate buffer solution for the bare SPCE and the modified SPCEs after aging are shown in Fig. 3a. For the bare SPCE, the anodic/cathodic peaks due to ferricyanide/ferricyanide were registered at 0.36/–0.15 V (as a hump), while for the modified SPCEs this redox system is shifted to 0.04/0.19 V for NIP-SPCE and 0.06/0.21 V for LPS-MIP-SPCE, where it is barely visible. The shift in the anodic/cathodic potential and the decrease in the current intensity suggested that the carbon surface of the SPCE became almost completely unavailable after film deposition, implying that surface modification occurred [18,19]. However, two other successive quasi-reversible redox systems due to ferricyanide/ferricyanide reaction at the interface with SiO₂/ZnO-based films appeared in the CVs of modified SPCEs. The LPS-MIP-SPCE registered anodic/cathodic peaks at 0.66 V/0.50 V and 0.90 V/0.80 V, while the NIP-SPCE peaks were at 0.66 V/0.40 V and 0.85 V/0.70 V. In contrast to the LPS-MIP-SPCE (Fig. 3b), the CV acquired for the NIP-SPCE (Fig. 3c) showed current intensities decreasing with each scan cycle, which, according to some authors, means that a poorly conducting interface was

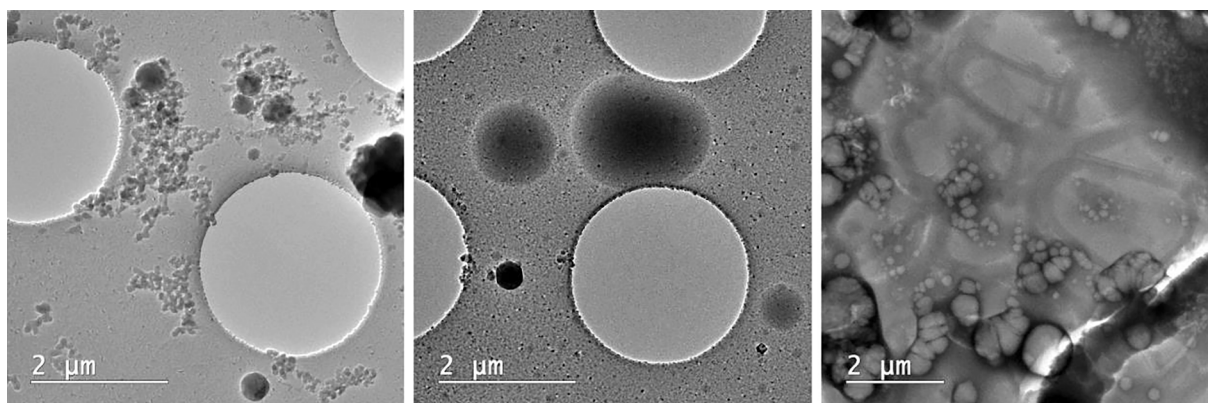


Fig. 1. Cryo-TEM micrographs of (A) LPS in water; (B) LPS in water + MAPTES; and (C) LPS in water + MAPTES + TEOS.

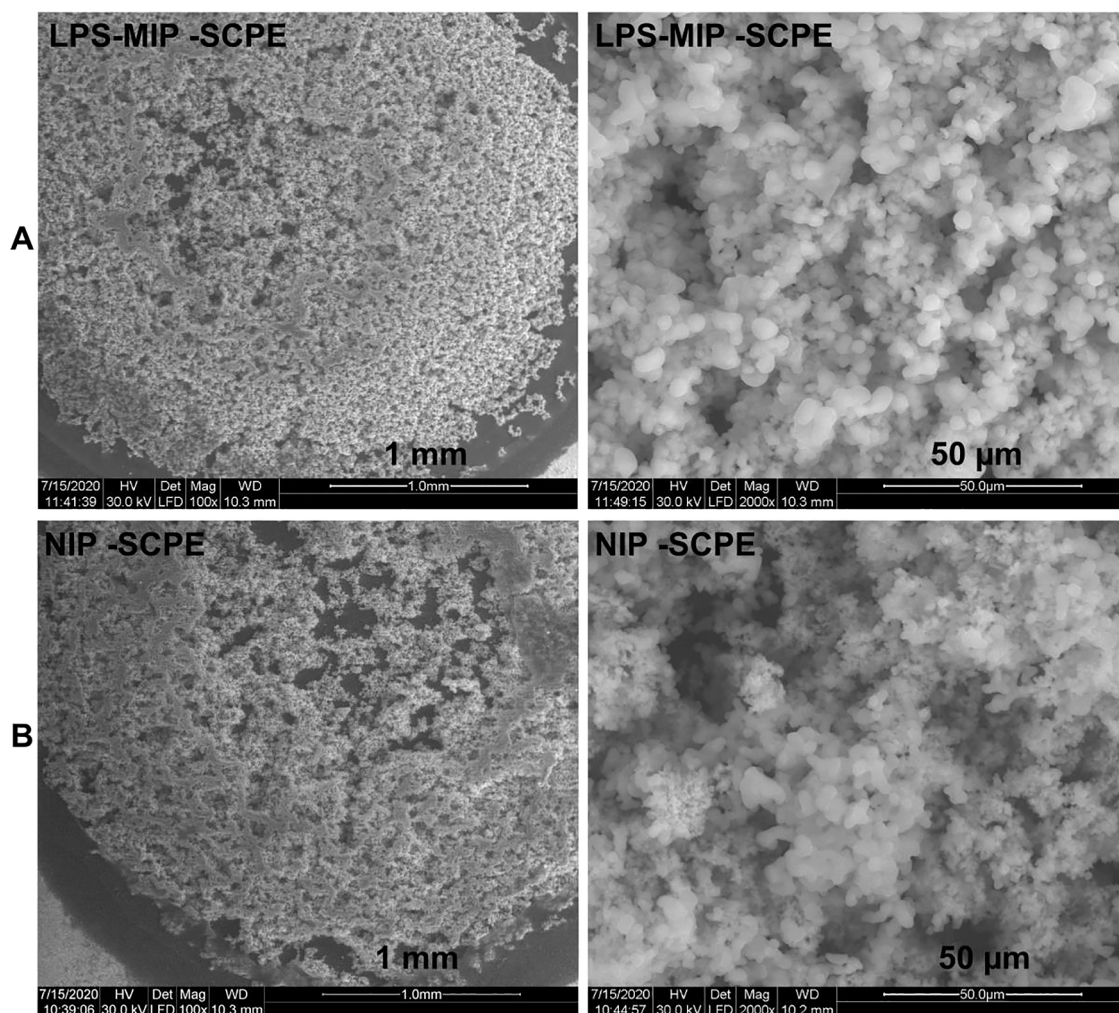


Fig. 2. SEM micrographs of (A) LPS-MIP-SPCE and (B) NIP-SPCE at different scales.

formed [19]. In this case, the SEM and BET results on the NIP-SPCE also indicated slow diffusion of the electrolyte, caused by the limited surface area and unsatisfactory pore structures.

After template extraction/washing, the current intensities of the peaks increased for both the LPS-MIP-SPCE (Fig. 4a) and the NIP-SPCE (Fig. 5a), as the surface of the films became more available to the electrolyte. In this step, the anodic/cathodic peaks registered at 0.66 V/0.50 V for the LPS-MIP-SPCE disappear and the ones at 0.66 V/0.40 V for

the NIP-SPCE are barely visible. This behavior is somewhat odd, but explicable in terms of the different polymer structures that may form [18]. The fact that the first redox system disappears almost completely after washing can be linked to the removal of non-condensed sols that can be detached easily from the surface during washing.

Further interesting behavior was observed after washing, this time affecting the second redox system, presumed to be characteristic of the oxidation/reduction of ferricyanide/ferrocyanide at the interface of the

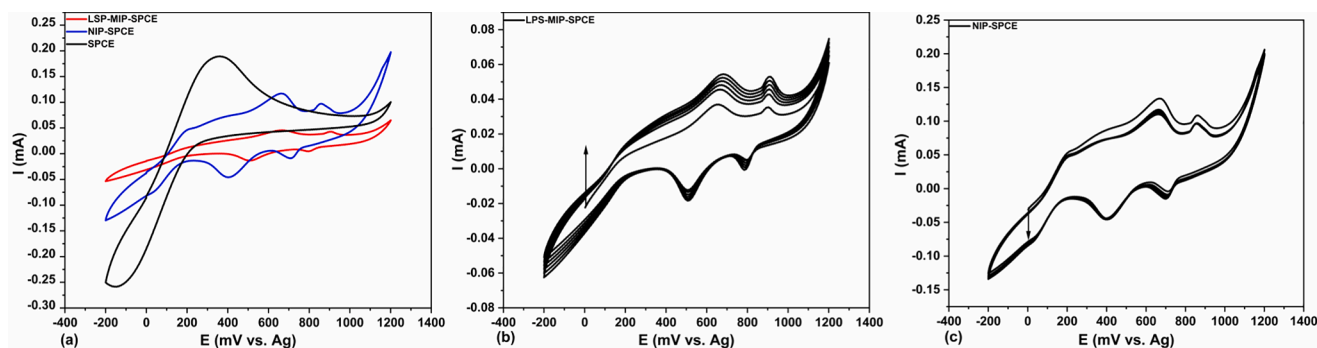


Fig. 3. CVs of: (a) bare SPCE, LPS-MIP-SPCE and NIP-SPCE; (b) LPS-MIP-SPCE over six scan cycles; and (c) NIP-SPCE during six scan cycles in 0.01 M $K_3[Fe(CN)_6]$ / $K_4[Fe(CN)_6]$ and 0.1 M KCl in PBS with pH 7.4, $\nu = 100$ mV/s, oxidation (right)/reduction (left) according to the IUPAC convention.

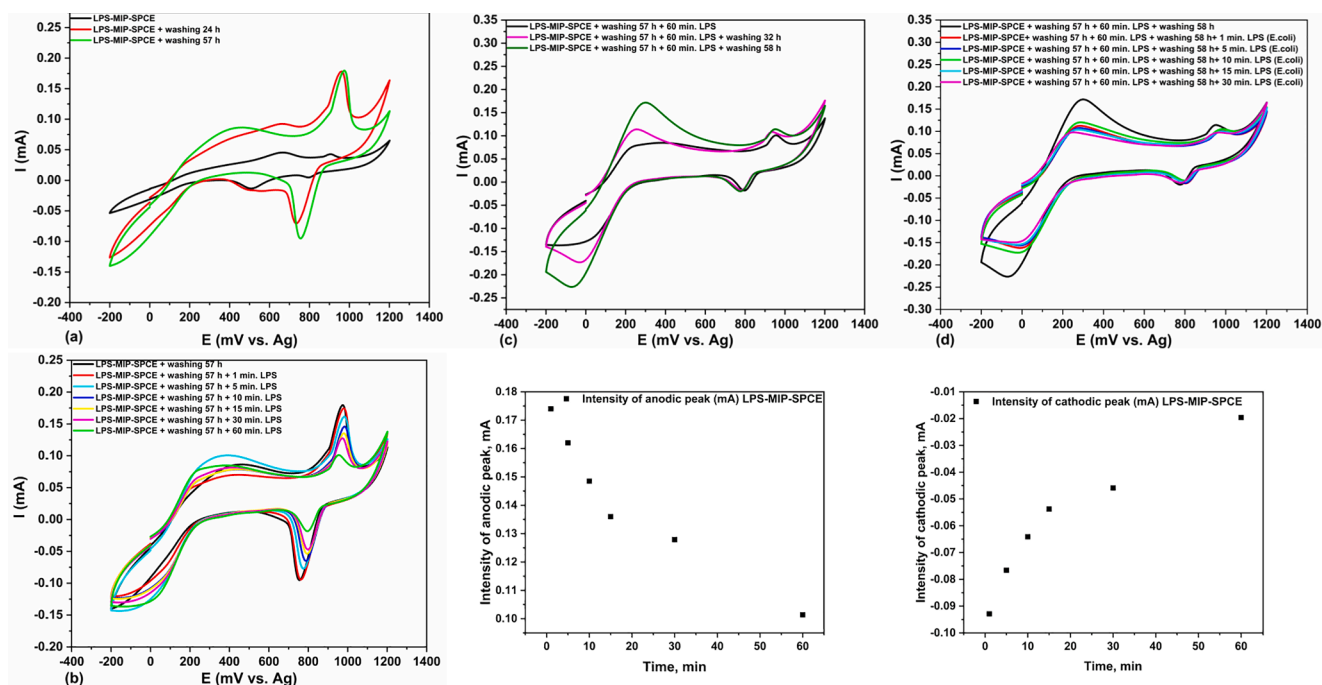


Fig. 4. CVs of the LPS-MIP-SPCE recorded in the following sequence: (a) during 57 h of washing/LPS extraction; (b) during 60 min of contact with LPS (*Pseudomonas Aeruginosa*) and the changes in the anodic/cathodic current intensities over time; (c) during 58 h of washing/LPS extraction; (d) during 30 min of contact with LPS (*Escherichia coli*) in 0.01 M $K_3[Fe(CN)_6]$ / $K_4[Fe(CN)_6]$ and 0.1 M KCl in PBS at pH 7.4, $\nu = 100$ mV/s, oxidation (right)/reduction (left) according to the IUPAC convention.

SiO/ZnO-based films. This time, however, a significant increase in the current intensities was noted. The LPS-MIP-SPCE registered an increase in the current intensity for the anodic (cathodic) peak of 0.18 mA (−0.10 mA), while the NIP-SPCE registered an increase of only 0.09 mA (−0.10 mA) (Fig. 5a), relative to same SPCEs before washing. Hence, it may be assumed that the 0.09 mA difference at the anodic peak between the LPS-MIP-SPCE and the NIP-SPCE is due to the removal of LPS from the structure of the film, which led to better diffusion of the electrolyte to the electrode surface as the imprinted cavities were cleaved [20]. This hypothesis was also sustained by the increase in the BET surface area after extraction of LPS.

The specificity test involved contacting the SPCEs with an aqueous solution of LPS from *Pseudomonas Aeruginosa* (166,667 U.E./mL or 16.7 μ g/mL) for up to 60 min (Figs. 4b and 5b). Electrochemical measurements were performed at 1, 5, 10, 15, 30, 60 min. After 1 min, the current intensity of the anodic (cathodic) peak for the LPS-MIP-SPCE started to decrease from its initial value, 0.18 mA (−0.10 mA), and reached about 0.10 mA (−0.02 mA) after 60 min in contact with LPS (Fig. 4b). Similar behavior was observed for the NIP-SPCE, with the

difference that the current intensity of the anodic (cathodic) peak decreased from 0.19 mA (−0.11 mA) and reached 0.14 mA (−0.07 mA) after 60 min in contact with LPS (Fig. 5b). Hence, the intensity difference, $\Delta I_A(\Delta I_C)$, for the LPS-MIP-SPCE was around 0.08 mA (−0.08 mA), while the corresponding figures for the NIP-SPCE were 0.05 mA (−0.04 mA). These values suggested that the LPS-MIP-SPCE detected LPS (from *Pseudomonas Aeruginosa*) more specifically than the control, NIP-SPCE.

During the second washing/extraction cycle the current intensities of the anodic/cathodic peaks increased again but only for the LPS-MIP-SPCE (Fig. 4c). The current intensity of the anodic (cathodic) peak for the LPS-MIP-SPCE increased to 0.11 mA (−0.02 mA), while that of the NIP-SPCE decreased to 0.13 mA (−0.04 mA) (Fig. 5c). In addition, a hump formed after extensive washing, which had a clear resemblance to the bare SPCE (Fig. 3a). Although this suggested that some of the particles may have been removed from the surface of the electrode, the same SPCEs were used for the selectivity study, in order to have comparable results with the earlier specificity study. In this case, an aqueous solution of LPS from *Escherichia coli* (166,667 U.E./mL or 16.7 μ g/mL) was tested.

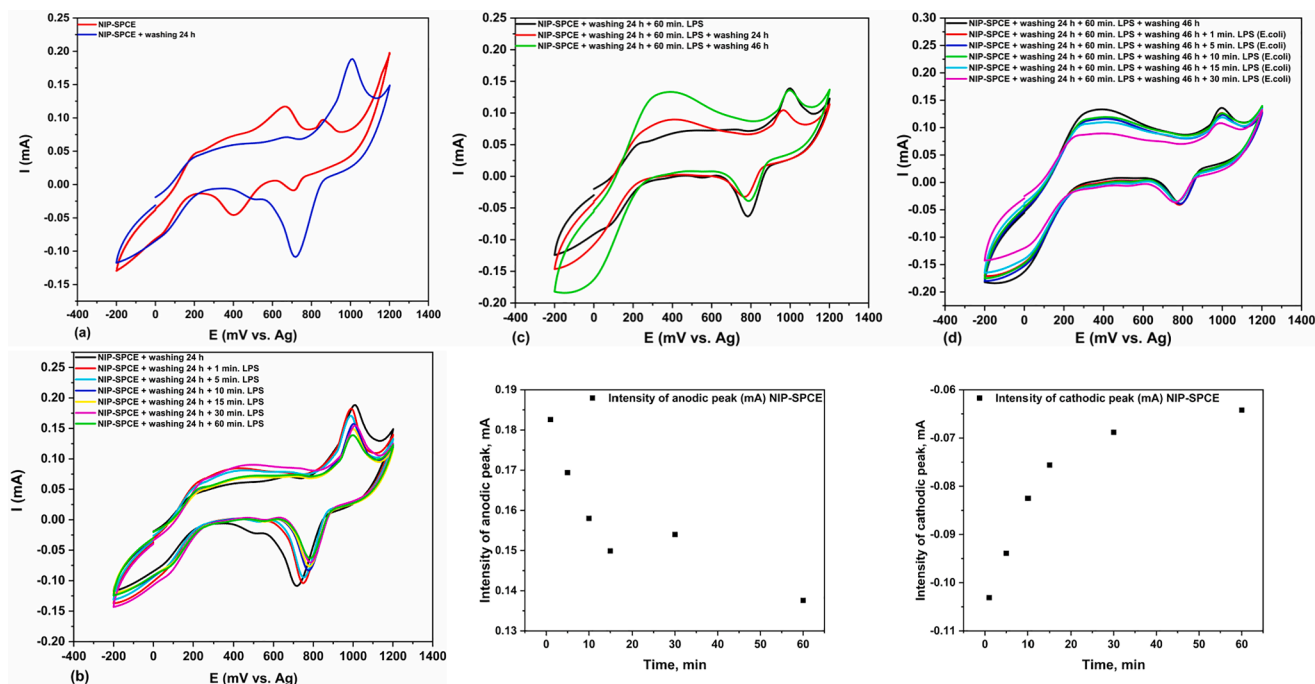


Fig. 5. CVs of the NIP-SPCE recorded in the following sequence: (a) during 24 h of washing; (b) during 60 min of contact with LPS (*Pseudomonas Aeruginosa*) and the changes in the anodic/cathodic current intensities over time; (c) during 46 h of washing/LPS extraction; (d) during 30 min of contact with LPS (*Escherichia coli*) in 0.01 M $K_3[Fe(CN)_6]/K_4[Fe(CN)_6]$ and 0.1 M KCl in PBS at pH 7.4, $\nu = 100$ mV/s, oxidation (right)/reduction (left) according to the IUPAC convention.

As observed in the previous case with LPS from *Pseudomonas Aeruginosa*, the intensity of the anodic (cathodic) peaks decreased for both modified SPCEs (LPS-MIP-SPCE in Fig. 4d and NIP-SPCE in Fig. 5d). However, during the entire period studied (30 min), the current intensities varied very little. ΔI_A (ΔI_C) was around 0.014 mA (-0.005 mA) for the LPS-MIP-SPCE and 0.016 mA (-0.004 mA) for the NIP-SPCE, suggesting that the response to LPS from *Escherichia coli* was quite different from that to LPS from *Pseudomonas Aeruginosa*.

It should also be noted that the NIP-SPCE registered decreasing intensities of currents with each scan cycle during all four experiments (i. e. first washing cycle, LPS detection from *Pseudomonas Aeruginosa*, second washing cycle and LPS detection from *Escherichia coli*), while the LPS-MIP-SPCE registered decreasing intensities of currents only during the LPS washing/extraction procedures. This observation suggests that re-binding of the LPS switched on the electrochemical behavior of the LPS-MIP-SPCE.

4. Conclusions

This study provides new insights into the fabrication of MIP-modified SPCEs with electrochemical features directed toward the detection of bacterial endotoxins (LPS) from *Pseudomonas Aeruginosa* [21]. The morphology and porosity analyses of the prepared LPS-MIP interfaces were consistent with the electrochemical behavior of the LPS-MIP-SPCEs. Considerable differences were observed between the LPS-MIP-SPCE and the control NIP-SPCE, after which it was concluded that the LPS-MIP-SPCE was able to recognize and re-bind the LPS from *Pseudomonas Aeruginosa* to a greater extent than the LPS from *Escherichia coli*, when using aqueous LPS solutions of 166,667 E.U./mL (16.7 $\mu\text{g}/\text{mL}$). In addition, the LPS-MIP interfaces demonstrated stability at re-use (covering at least two reconditioning cycles). Considering the interesting discoveries described in this study, together with the fact that no reports of such biosensors for LPS have so far been published (to the best of our knowledge), we can say that this pioneering study serves as a starting point for the development of original and selective biosensors able to detect bacterial endotoxins; and, hence, the probable presence of

pathogenic bacteria in various aqueous systems or even biological fluids. As the amount of endotoxins may vary from region to region and the source of the water (from 0.004 E.U./mL in bottled water to 183,000 E.U./mL in primary wastewater [22]), the developed LPS biosensor design is suitable for detecting LPS in highly charged water effluents.

CRedit authorship contribution statement

Bianca Elena Stoica: Investigation, Writing - original draft. **Ana-Mihaela Gavrilă:** Methodology, Investigation. **Andrei Sarbu:** Supervision, Writing - review & editing. **Horia Iovu:** Supervision, Writing - review & editing. **Hugues Brisset:** Supervision, Writing - review & editing. **Andreea Miron:** Investigation. **Tanta-Verona Iordache:** Conceptualization, Writing - original draft, Project administration, Funding acquisition, Resources, Writing - review & editing.

Declaration of Competing Interest

The authors declare that they have no known competing financial interests or personal relationships that could have appeared to influence the work reported in this paper.

Acknowledgement

The study was funded by the Ministry of Education and Research through UEFISCDI [project no. TE 123/2018-BACTERIOSENS and project no. 255PED/2020 TOXINSENS]. The authors thank Dr. Bogdan Trica and Dr. Elvira Alexandrescu from INCDCP-ICECHIM Bucharest for the morphology analysis.

References

- [1] C. Dye, Philos. Trans. R. Soc. B 369 (2014) 20130426.
- [2] L. Paruch, A.M. Paruch, H.G. Eiken, R. Sorheim, Sci. Rep. 9 (2019) 19469.
- [3] L. Váradi, J.L. Luo, D.E. Hibbs, J.D. Perry, R.J. Anderson, S. Orenga, P. W. Groundwater, Chem. Soc. Rev. 46 (2017) 4818–4832.
- [4] M. Cho, L. Chun, M. Lin, W. Choe, J. Nam, Y. Lee, Sens. Actuator B: Chem. 174 (2012) 490–494.

- [5] Z. Li, G. Dai, F. Luo, Y. Lu, J. Chu, P. He, F. Zhang, Q. Wang, *Microchim. Acta* 187 (2020) 415.
- [6] H. Jiang, J. Yang, K. Wan, D. Jiang, C. Jin, *ACS Sens.* 5 (2020) 1325–1335.
- [7] D. Antuna-Jimenez, M.B. Gonzalez-Garcia, D. Hernandez-Santos, P. Fanjul-Bolado, *Biosensors* 10 (2020) 9.
- [8] M.L. Yola, N. Atar, *Curr. Anal. Chem.* 13 (2017) 13–17.
- [9] R. Peltomaa, B. Glahn-Martinez, E. Benito-Pena, M.C. Moreno-Bondi, *Sensors* 18 (2020) 4126.
- [10] B. Cui, P. Liu, X. Liu, S. Liu, Z. Zhang, *J. Mater. Res. Technol.* 9 (2020) 12568–12584.
- [11] Y. Saylan, S. Akgönüllü, H. Yavuz, S. Ünal, A. Denizli, *Sensors* 19 (2019) 1279.
- [12] R. Gui, H. Jin, H. Guo, Z. Wang, *Biosens. Bioelectron.* 100 (2018) 56–70.
- [13] F. Cui, Z. Zhou, H.S. Zhou, *Sensors* 20 (2020) 996.
- [14] S. Löffler, H. Antypas, F.X. Choong, K. Peter, R. Nilsson, A. Richter-Dahlfors, *Front. Chem.* 7 (2019) 265.
- [15] S. Piletsky, F. Canfarotta, A. Poma, A.M. Bossi, S. Piletsky, *Trends Biotechnol.* 38 (2020) 368–387.
- [16] D.B. Kell, E. Pretorius, (Perspective) *Integr. Biol.* 7 (2015) 1339–1377.
- [17] A.M. Gavrila, A. Zaharia, L. Paruch, F.X. Perrin, A. Sarbu, A.G. Olaru, A.M. Paruch, T.V. Iordache, *J. Hazard. Mater.* 399 (2020), 123026.
- [18] B.E. Georgescu, C. Branger, T.-V. Iordache, H. Iovu, O.B. Vitrik, A.V. Dyshlyuk, A. Sarbu, H. Brisset, *Electrochem. Commun.* 94 (2018) 45–48.
- [19] Y. Li, Y. Liu, J. Liu, J. Liu, H. Tang, C. Cao, D. Zhao, Y. Ding, *Sci. Rep.* 5 (2015) 7699.
- [20] B. Feier, A. Blidar, A. Pusta, P. Carciuc, C. Cristea, *Biosensors* 9 (2019) 31.
- [21] T.V. Iordache, E.B. Stoica, A. Sârbu, A.M. Gavrila, A.-L. Ciurlică, A.L. Chiriac, A. Zaharia, T. Sandu, O.S.I.M., RO Patent Application, A2019-0804, 2019.
- [22] C. Zhang, F. Tian, M. Zhang, Z. Zhang, M. Bai, G. Guo, W. Zheng, Q. Wang, Y. Shi, L. Wang, *Sci. Total Environ.* 681 (2019) 365–378.